DETECTING NANOPHASE WEATHERING PRODUCTS WITH CHEMIN: REFERENCE INTENSITY RATIOS OF ALLOPHANE, ALUMINOSILICATE GEL, AND FERRIHYDRITE.

E. B. Rampe[1,2], D. L. Bish[3], S. J. Chipera[4], R. V. Morris[1], C. N. Achilles[1], D. W. Ming[1], D. F. Blake[5], R. C. Anderson[6], T. F. Bristow[5], J. A. Crisp[6], D. J. Des Marais[5], R. T. Downs[7], J. D. Farmer[8], J. M. Morookian[6], S. M. Morrison[7], P. Sarrazin[9], N. Spanovich[6], E. M. Stolper[10], A. H. Treiman[11], D. T. Vaniman[12], A. S. Yen[6], and the MSL Science Team, [1]NASA JSC Houston, TX 77058, elizabeth.b.rampe@nasa.gov, [2]Oak Ridge Associated Universities Oak Ridge, TN 37830, [3]Indiana Univ., [4]CHK Energy, [5]NASA ARC, [6]JPL, [7]Univ. of Arizona, [8]Arizona State Univ., [9]In-Xitu, [10]Caltech, [11]LPI, [12]PSI.

Introduction: X-ray diffraction (XRD) data collected of the Rocknest samples by the CheMin instrument on Mars Science Laboratory suggest the presence of poorly crystalline or amorphous materials [1], such as nanophase weathering products or volcanic and impact glasses. The identification of the type(s) of X-ray amorphous material at Rocknest is important because it can elucidate past aqueous weathering processes. The presence of volcanic and impact glasses would indicate that little chemical weathering has occurred because glass is highly susceptible to aqueous alteration. The presence of nanophase weathering products, such as allophane, nanophase iron-oxides, and/or palagonite, would indicate incipient chemical weathering. Furthermore, the types of weathering products present could help constrain pH conditions and identify which primary phases altered to form the weathering products.

Quantitative analysis of phases from CheMin data is achieved through Reference Intensity Ratios (RIRs) and Rietveld refinement. The RIR of a mineral (or mineraloid) that relates the scattering power of that mineral (typically the most intense diffraction line) to the scattering power of a separate mineral standard such as corundum [2]. RIRs can be calculated from XRD patterns measured in the laboratory by mixing a mineral with a standard in known abundances and comparing diffraction line intensities of the mineral to the standard. X-ray amorphous phases (*e.g.*, nanophase weathering products) have broad scattering signatures rather than sharp diffraction lines. Thus, RIRs of X-ray amorphous materials are calculated by comparing the area under one of these broad scattering signals with the area under a diffraction line in the standard. Here, we measured XRD patterns of nanophase weathering products (allophane, aluminosilicate gel, and ferrihydrite) mixed with a mineral standard (beryl) in the CheMinIV laboratory instrument and calculated their RIRs to help constrain the abundances of these phases in the Rocknest samples.

Methods: Allophane, aluminosilicate gel, and ferrihydrite were synthesized in the laboratory according to methods in [3-5]. Allophane with Si/Al molar ratios of 0.44 and 0.92, aluminosilicate gel with a Si/Al ratio of 5.6, and two-line ferrihydrite were freeze-dried to produce fine powders. Allophane with an Si/Al ratio of 0.61 was air dried, then ground in an agate mortar and pestle, and sieved to 45-90 μm to examine effects that particle size may have on movement in the CheMin cell and, thus, on the measured RIRs. These synthesized materials were each mixed with a beryl standard in 50:50 weight proportions. Freeze-dried materials were mixed with <45 μm beryl and the air-dried allophane was mixed with 45-90 μm beryl. The mixtures were measured in the CheMinIV instrument at NASA Johnson Space Center, which is a laboratory testbed for CheMin on MSL. RIRs of each nanophase weathering product were determined by measuring the area under the beryl peak at 12.8° 2θ and under the X-ray amorphous low-angle intensity rise from 4-10° 2θ [2]. RIRs of nanophase weathering products were measured using the area under the low-angle rise as opposed to the amorphous hump because the area under the amorphous humps are small compared with the areas under the low-angle rises and thus offer a more robust value and can be readily distinguished from the amorphous hump of the basaltic glass that also occurs in the Rocknest samples. As corundum is the normal standard used in RIR measurements, the reported RIRs were converted to a corundum reference using the RIR of 1.70 (beryl:corundum 50:50 mixture) measured on a laboratory Bruker XRD instrument.

Results and Discussion: CheMinIV patterns of allophane mixed with beryl show sharp diffraction lines from beryl and very broad, low-intensity humps ~20-35° 2θ and ~43-52° 2θ and a low-angle rise <15° 2θ (Figure 1). The pattern of aluminosilicate gel is similar to those of allophane, but the hump at ~43-53° 2θ in the aluminosilicate gel pattern is much weaker than that in the allophane patterns. Weakly altered natural basaltic glass patterns display a low-angle rise and low-intensity amorphous hump ~20-35° 2θ similar to those in allophane and aluminosilicate gel patterns [6]. The CheMinIV pattern of ferrihydrite mixed with beryl shows a broad, low-intensity hump ~30-45° 2θ and a steep low-angle rise <10° 2θ (Figure 2). The low-angle rise in ferrihydrite differs from those in allophane and

aluminosilicate gel because the ferrihydrite rise is steeper, begins at lower angles, and has a greater area under the curve. The measured RIRs for each nanophase weathering product are listed in Table 1. Particle segregation due to particle size does not appear to occur or affect measured RIRs as the RIR of the 45-90 μm allophane (Si/Al = 0.61) is similar to that of the fine powder allophane (Si/Al = 0.92). If particle segregation had occurred, we would expect differences in the areas under the low-angle rise and the 12.8 °2θ beryl peak between the allophane samples resulting from differences in allophane vs. beryl contributions to the patterns. We are continuing to investigate the effects of particle segregation within the CheMinIV cell on patterns collected over the course of a sample measurement.
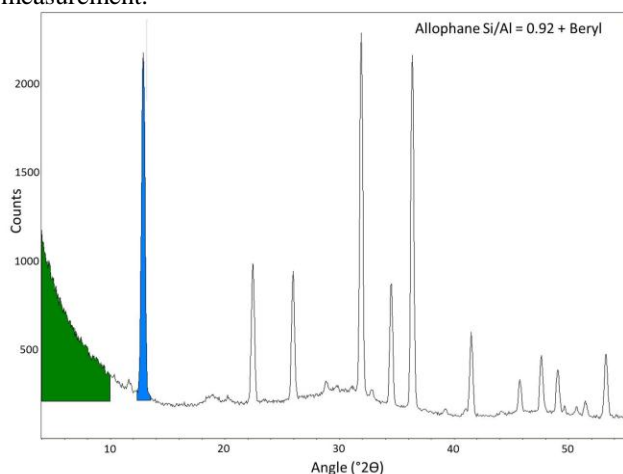
Figure 1. CheMinIV XRD pattern of allophane (Si/Al = 0.92) mixed with beryl (50:50 wt.). The area shaded in green represents the area under the low-angle rise caused by allophane used for RIR measurements. The area shaded in blue represents the area under the beryl peak used for RIR measurements.
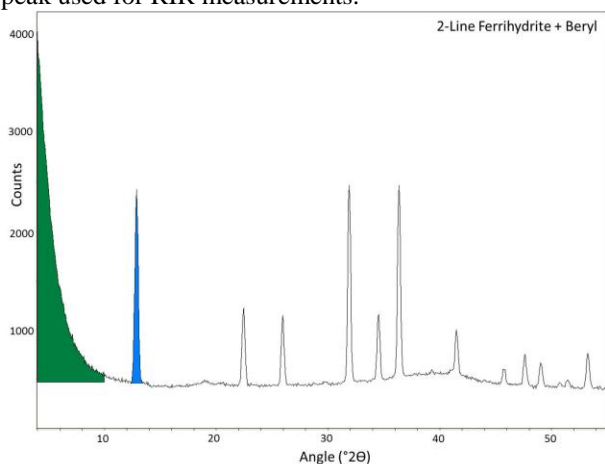
Figure 2. CheMinIV XRD pattern of two-line ferrihydrite mixed with beryl (50:50 wt.). The area shaded in

green represents the area under the low-angle rise caused by ferrihydrite used for RIR measurements. The area shaded in blue represents the area under the beryl peak used for RIR measurements.

Table 1. RIRs of nanophase weathering products.

Sample	RIR
Allophane Si/Al = 0.44	4.5
Allophane Si/Al = 0.61	5.9
Allophane Si/Al = 0.92	6.3
Aluminosilicate gel Si/Al = 5.6	6.1
Ferrihydrite	13.8

The evidence for the presence of poorly crystalline or amorphous materials in CheMin data from Rocknest is an elevated background from 15-40° 2θ and a low-angle rise <~6° 2θ not seen with empty cells [1]. Quantitative analyses of Rocknest data suggest that this material consists mainly of a glassy component with minor amounts of a poorly crystalline aluminosilicate [7]. Similarities between XRD patterns of poorly crystalline and amorphous phases create difficulties in characterizing these phases in martian (and terrestrial) samples. However, small differences in the position and slope of the low-angle rise and the position of the amorphous hump(s) allow for some distinction between poorly crystalline aluminosilicates and ferrihydrite in CheMin data and in their measured RIRs. Further analyses of the amorphous and poorly crystalline materials and their relative abundances in martian soils as the MSL mission proceeds will answer outstanding questions about the aqueous alteration environment and the local differences or homogeneity of martian soils.

References: [1] Blake D. F. et al. (2013) *LPS XLIV,* Abstract #A. [2] Snyder R. L. and Bish D. L. (1989) *Reviews in Mineralogy, 104,* 44. [3] Wada S. I. et al. *J. Soil Sci., 30,* 347-355. [4] Ohashi F. et al. (2002) *Clay Min., 37,* 451-456. [5] Schwertmann U. and Cornell R. M. (1991) *Iron Oxides in the Laboratory.* [6] Achilles C. N. et al. (2013) *LPS XLIV,* Abstract #B. [7] Bish D. L. et al. (2013) *LPS XLIV,* Abstract #C.